Solid Freeform Fabrication 2022: Proceedings of the 33rd Annual International Solid Freeform Fabrication Symposium – An Additive Manufacturing Conference
Reviewed Paper

INVESTIGATION OF THE PROCESS PARAMETERS AND GEOMETRY DEPENDENT SHRINKAGE BEHAVIOR OF RASTER LINES IN THE FUSED DEPOSITION MODELING PROCESS

E. Moritzer*, F. Hecker*†

*Kunststofftechnik Paderborn (KTP), Paderborn University, Germany
*Direct Manufacturing Research Center (DMRC), Paderborn University, Germany
†Corresponding author

Abstract

Additive Manufacturing processes are able to generate components from raw material (filament, powder etc.) without the need of tools or conventional machining. One of the most common Additive Manufacturing processes is the Fused Deposition Modeling (FDM). Here, a thermoplastic polymer filament is fed into a heated nozzle where the filament is plasticized. The plasticized material is then deposited, layer-by-layer onto the building platform or the already existing component structure in a defined way. Thermoplastic polymers show a material specific shrinkage induced by the cooling process. The recurring heat input by depositing adjacent strands results in a complex cooling situation which contributes to the non-uniform shrinkage of the component. In the investigations, first, a Design of Experiments (DoE) is carried out to determine the influence of selected process parameters on the shrinkage behavior of the raster lines. Following, the geometrical deviations of simple geometries under consideration of different process parameters are determined and analyzed.

Introduction

In this paper the influence of selected process parameters on the shrinkage behavior of raster lines in the FDM process was investigated. This was done using a DoE software (Design-Expert 12) to evaluate the influences and interactions of different factors on the geometrical deviation of specimens. For this, the raster lines were oriented in direction of the specimen's nominal length. To be able to utilize the results of this study for further investigation, the standard raster sequence angle of 90° relative to the raster angle of the previous layer was applied. A Stratasys Fortus 400mc was used to manufacture the specimens. The specimens were precisely measured using a coordinate measuring machine. Based on the results, a function was determined to describe the shrinkage behavior depending on the selected process parameters and nominal lengths. This function was then used to calculate the expected geometrical deviation for randomized nominal lengths and process parameters to validate the modeling.

State of the Art

The Fused Deposition Modeling (FDM) currently is the most used Additive Manufacturing technology [1]. In 1989 the FDM technology was developed and patented by Stratasys [2]. As the FDM process is an Additive Manufacturing (AM) technology, it is based on the characteristic layer wise generation of components. For this, the FDM process processes a thermoplastic polymer filament which is stored on a spool. The filament is fed into a heated nozzle, where it is molten. By a precise positioning and traversing of the nozzle in the x-y-plane a molten thermoplastic polymer strand is deposited onto a building platform or an already

existing component structure. After the completion of a layer, the distance between the building platform and the nozzle tip in the z-direction is increased by one layer height.

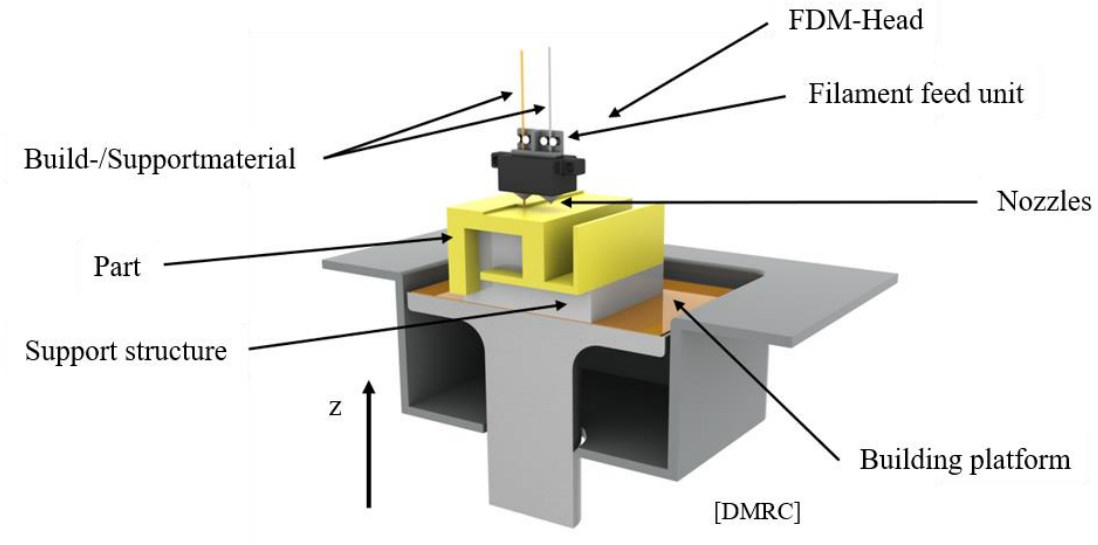

Figure 1: Schematic of the FDM process.

Following, the deposition process continues. This is repeated until the component is completed [3]. The machine principle is shown in Figure 1. When cooling down after processing, thermoplastic polymers show a characteristic shrinkage behavior. As the FDM process is a tool less technology the shrinkage cannot be prohibited by formative elements [4]. Currently this matter is addressed by applying linear compensation factors.

Research conducted by KNOOP shows that these linear compensation factors do not cover the complete range of manufacturable nominal lengths of the considered specimens. A DoE was conducted. The results show that in addition to process parameters (e.g. layer height, air gap, strand width/height ratio etc.) also the nominal length has an influence on the geometric deviations [5]. This suggests, that the application of linear shrinkage factors does not enable an optimal compensation of the occurring geometric deviations in the FDM process.

Research Approach

Based on the previous research, the investigations presented in this paper focus on the shrinkage behavior of raster lines in the FDM process. This approach is based on the FDM process being an extrusion process. Extrusion in the field of polymers is an established process which is closely related to injection molding. In the polymer extrusion process, material is plasticized using a screw. In contrast to the injection molding process, here, the material is continuously fed through a die to achieve the desired geometries [6]. As the FDM process is based on the principle of extrusion, it is assumed that effects observed in the polymer extrusion process are applicable.

Literature shows that during the extrusion process the molecular chains align in the direction of extrusion. This leads to anisotropic behavior of the material properties and therefore also of the part properties. In the direction of extrusion, the stiffness and also the strength are increased. But also, the thermal expansion and shrinkage increase. These effects are normally reversed due to the Brownian motion. Under certain circumstances, for example a fast cooling of the melt, the orientation and therefore the effects can partially remain [7].

In this research the shrinkage behavior of raster lines in the FDM process, depending on selected process parameters and the nominal length of the specimens, is investigated. The

influence of the nominal length on the geometric deviations of the specimens is analyzed and evaluated regarding linear behavior.

Experimental Investigations

The experimental investigations are based on a Design of Experiments (DoE). The DoE is used for the determination of the different influences and interactions of the selected process parameters. For this the software Design-Expert 12 is used. A fractional factorial face centered central composite design is chosen. The fractional factorial option enables the limitation of the necessary test points to 72 for each layer height. This includes three reproductions which result in overall 216 specimens for all three layer heights. A face centered design was chosen to be able to assure that no non-selectable process parameter combinations are requested for the DoE, as the slicing software (Insight) does only allow the process parameters to be set in certain boundaries. For the layer height, only certain values can be selected. Therefore, the layer height is defined as categorial factor. The considered factors are selected based on the results presented by KNOOP [5]. The parameters and the corresponding steps are shown in Table 1.

Table 1: Factors and corresponding factor steps selected for the conduction of the DoE.

Factor	**Steps**				
	1	**2**	**3**	**4**	**5**
Nominal length / mm	5	53.75	102.5	151.25	200
Raster angle / °	0	45	90	135	180
Air gap / %	0	-1.25	-2.5	-3.75	-5
w/h-ratio / -	1.7	2.025	2.35	2.675	3
Layer height / mm	0.1778	0.2540	0.3302	-	-

As specimen geometry, a cuboid shape is chosen. The specimens have a width and height of 10 mm. The specimen length is chosen according to the steps shown in Table 1. This is done because the deposition and measuring of a single deposited strand is not viable. Due to possible irregularities during the beginning and end of the deposition process, the length of the single deposited strand is falsified with a high probability. Therefore, the manufacturing of specimens which represent a strand compound structure is conducted.

To identify the shrinkage behavior and therefore the geometrical deviations of raster lines, the raster lines are aligned along the nominal length of the specimens. Therefore, the raster line decides the orientation of the specimens in the build chamber (see Figure 2).

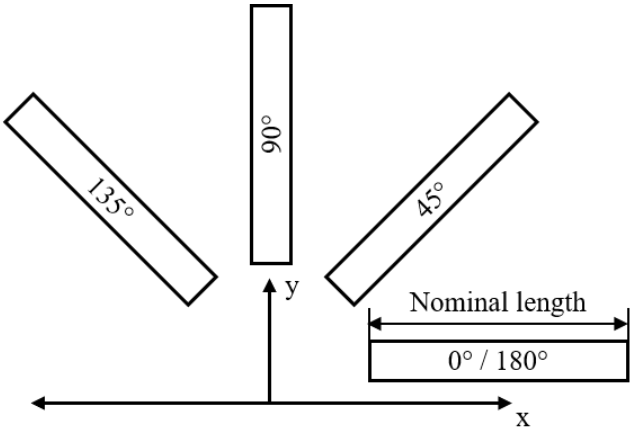

Figure 2: Orientation of the specimens in the build chamber according to the raster angles.

As the raster lines for the raster angles 0° and 180° are aligned identically, the same specimens and values are used during the evaluation. To consider the processing boundary conditions applicable for standard components manufactured with the system, a raster sequence angle of 90° is applied. This means that in only every second layer the raster lines are oriented in the direction of the nominal length of the specimens.

The parameters air gap, width/height-ratio (w/h-ratio) of the strands and layer height are linked. All parameters are based on the specific layer height which determines the height for the w/h-ratio. The corresponding strand width is calculated based on the steps in Table 1. The air gap is then calculated for each of the applicable strand widths.

The air gap describes the distance between the deposited strands and is specified in millimeters. For these investigations, the air gap is defined in percent of the chosen strand width. This specification relative to the strand width improves the comparability between different layer heights. Only negative air gaps are considered as the investigations of KNOOP did not show a significant influence of positive air gaps [5].

For the manufacturing of the specimens, the positioning on the building platform is assigned randomly. For each layer height, three separate build jobs are prepared and manufactured. After manufacturing, the specimens are removed from the building platform and left to cool down for at least 24 h at standard climate (21 °C / 50 % rel. humidity).

To measure the specimens, they are fixed onto a platter on a NIKON Altera 8.7.6 coordinate measuring machine (see Figure 3). The measuring software Camio 8.4. is used. All specimens are measured using a tactile measuring probe (2 mm sphere diameter).

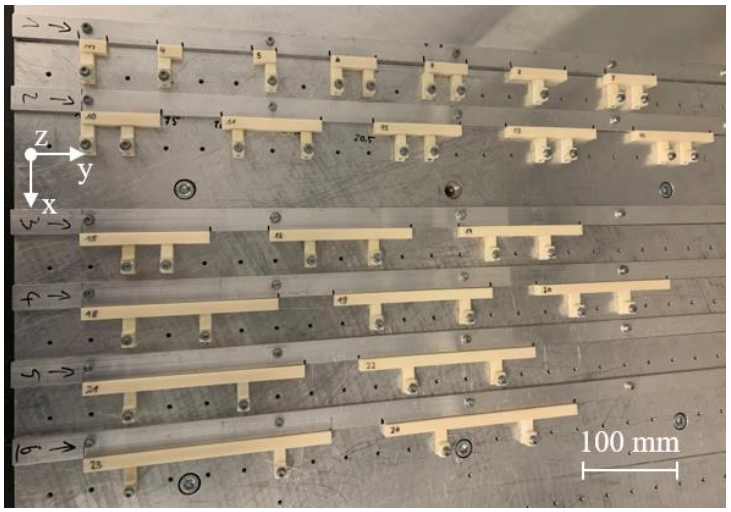

Figure 3: Specimens of one build job fixed onto the platter of the coordinate measuring machine.

For the measurement of the geometric deviation and therefore the shrinkage of the specimens, the front and back surface are measured. This is done by measuring five points on each of the surface. This results in five pairs of measured points of which each pair has identical x- and z- coordinates (see Figure 4).

These points cover an area of 4 mm x 4 mm in the center of the surface. Due to effects such as the weld line or irregularities caused by redirecting the strand in the corner areas, the border surrounding the square is not considered. To determine the specimen length, the difference of the y-coordinates for each pair is calculated. This results in five values for each specimen of which the average value is determined. By using this method, a more detailed evaluation of the geometric deviations is possible. The specimens with a nominal length of 5 mm are measured using an outside micrometer as they could not be fixed to the platter of the

coordinate measuring machine and therefore are only represented by a single value for each specimen.

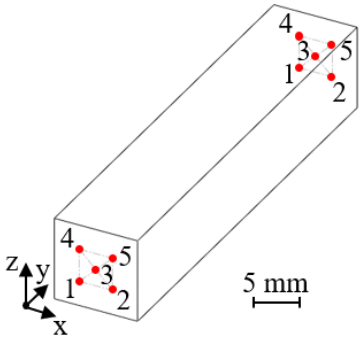

Figure 4: Positions of the measuring points (red) on the front and back surface of the specimens.

As many process parameter combinations are used to manufacture the specimens, the overall results are only evaluated using the DoE software (Design-Expert 12). During the further investigations a phenomenon present in every specimen is observed. The measurements of the front and back surface show a curvature of these surfaces. This curvature is exaggeratedly shown in Figure 5.

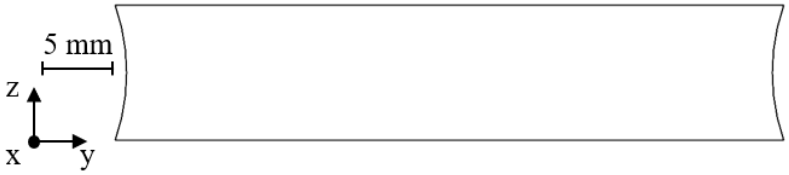

Figure 5: Exaggerated depiction of the occurring curvature of the front and back surface of the specimens.

To further investigate this phenomenon, additional specimens with a height of 30 mm are manufactured. This results in a bottom, a middle and a top section of 10 mm in height each. The width of the specimens is kept at 10 mm and the nominal lengths shown in Table 1, except for the 5 mm specimens, are used. The process parameters are set as shown in Table 2. Here, too, the specimens are aligned to the raster angle and oriented accordingly in the build chamber. For each layer height, three specimens for each nominal length are manufactured. This results in a total of 36 specimens. These are then, analog to the previous specimens, measured using a coordinate measuring machine. For the measurements, the measuring points shown in Figure 4 are used and applied to the bottom, middle and top section (see Figure 6) with each of the 4 x 4 mm^2 measuring areas being surrounded by a 3 mm border.

Table 2: Process parameters for the manufacturing of the specimens to investigate the curvature.

Process parameters			
Layer height / mm	0.1778	0.2540	0.3302
Strand width / mm	0.3556	0.5080	0.6604
Air gap / mm	0		
Raster angle / °C	45		

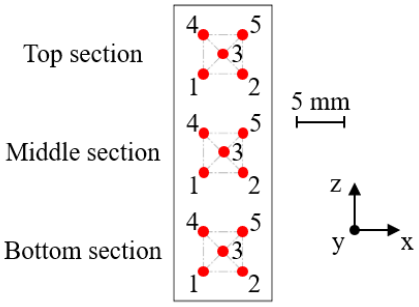

Figure 6: Positioning of the measuring points (red) for the specimens with a height of 30 mm.

Results and Discussion

After manufacturing and measuring of the specimens the measured geometrical deviations are entered into the DoE software. A quadratic model is suggested by the DoE software. The model is not optimized as with every attempt the initial R^2-value of 0.9792 decreases. In the following only the influences of the nominal length, raster angle, air gap, w/h-ratio and layer height are described and interpreted. The graphs shown in Figures 7 - 11 are based on the combination of a nominal length of 100 mm, a raster angle of 90°, an air gap of 2.525 %, a w/h-ratio of 2.35 and a layer height of 0.1778 mm.

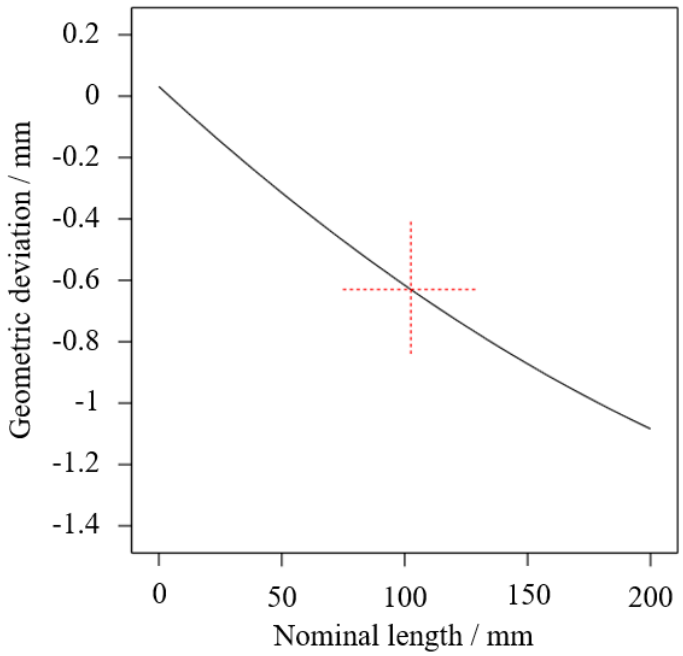

Figure 7: Effect of the nominal length on the geometric deviation.

According to the results shown in Figure 7 - 11 the nominal length is the most significant influence factor on the geometric deviation of the specimens. The graph in Figure 7 is based on a linear and a quadratic component which results in a slight curve of the graph. The coefficients given in the equation for the linear and quadratic component are -0.2932 and 0.0213 respectively. Therefore, the influence of the quadratic component is significantly smaller.

The graph shown in Figure 8 shows the influence of the raster angle on the geometric deviation. As specimens manufactured with a raster angle of 0° are identical to those manufactured with a raster angle of 180°, these points share identical geometric deviations. The

graph shows a symmetrical course with a raster angle of 90° showing the highest geometric deviation. A possible explanation for this is that the x- and y-axis do not perform the exact same travel movements. This may be induced by the belt drives powering the x- and y-axis not being identical. Caused by the rectilinear shape of the building platform and the resulting greater range of action for the x-axis, the belt powering the x-axis is longer. To achieve an ideal coordination of the axis movements, the machine is calibrated. A faulty calibration may be an explanation for the results shown in Figure 8.

The investigations of KNOOP did not show a significant influence of positive air gaps on the geometric deviations. The graph in Figure 9 does not show a notable influence of negative air gaps. Based on the results of KNOOP, a minimum air gap of -5 % was chosen as

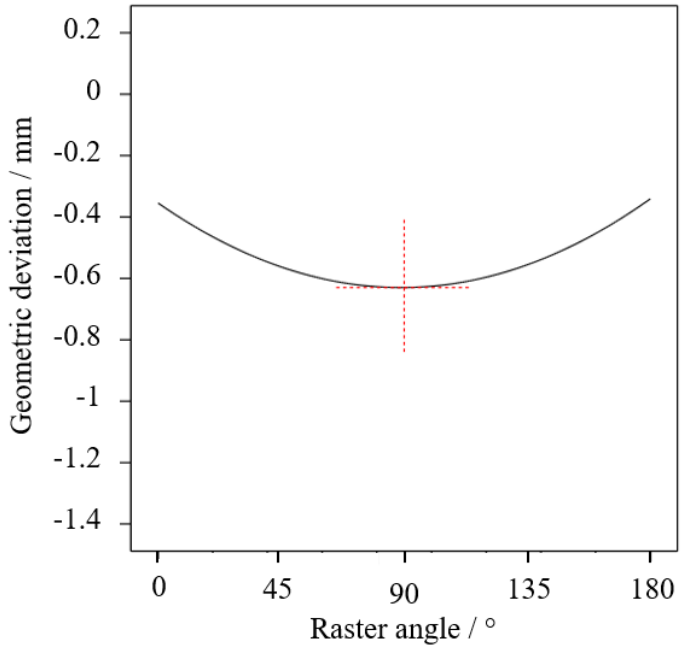

Figure 8: Effect of the raster angle on the geometric deviation.

lower values lead to an overfilling of the parts, which is not desired in standard applications and therefore not investigated during this research [5]. With a linear coefficient of 0.0009 and a quadratic coefficient of 0.0035 the air gap does not have a significant influence on the geometric deviation. The air gap does only alter the distance between the raster lines. As the alteration is comparably small, possible effects may have not been detected. For these investigations, effects occurring at an even lower air gap and overfilled parts are not relevant and are therefore not further considered.

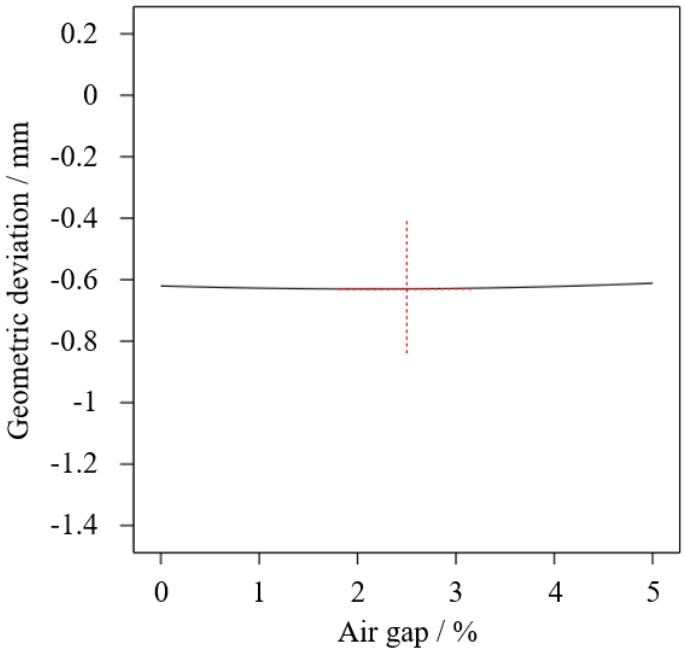

Figure 9: Effect of the air gap on the geometric deviation.

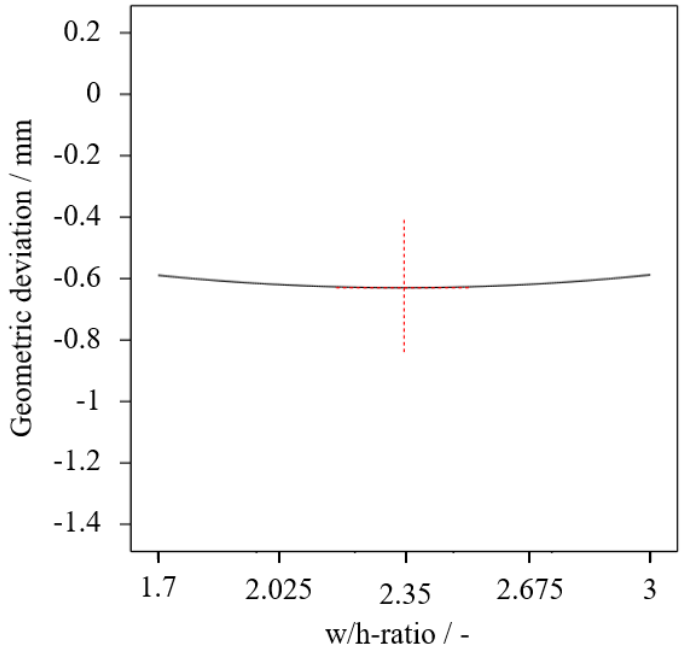

Figure 10: Effect of the w/h-ratio on the geometric deviation.

Figure 10 shows the effect of the w/h-ratio on the geometric deviation of the specimens. The diagram shows a quadratic effect with the highest deviation occurring in the center of the considered range of the w/h-ratio. A possible explanation for this is, that with a higher w/h-ratio the diameter of the deposited strand and therefore the volume extruded in a defined time interval increases, if the print velocity is kept constant. A further investigation has the aim to determine the volume flow rate of the material exiting the nozzle. For this, two identical specimens were manufactured using the process parameters shown in Table 3.

Table 3: Parameters for manufacturing of the specimens for the further investigation of the w/h-ratio.

Specimen	**1**	**2**
w/h-ratio / -	1.7	3
Layer height / mm	0.2540	
Strand width / mm	0.4318	0.7620

As specimens, cuboids with a length of 150 mm and a height and width of 10 mm each are manufactured. The raster lines are aligned along the length of 150 mm. This results in 21 raster lines for the specimen with the lower w/h-ratio (specimen 1) and 11 raster lines for the specimen built with a w/h-ratio of 3 (specimen 2). To calculate the volume flow rate for both w/h-ratios, the time for the completion of a single layer is measured. Combined with the calculated cross-section of the strands, which is assumed to be an ellipse (see (1)), the volume flow rate is determined. The values are shown in Table 4.

$$A = \left(\frac{layer\ height}{2}\right) * \left(\frac{strand\ width}{2}\right) * \pi \qquad (1)$$

As the nozzle diameter is constant, the velocity of the material flowing through the nozzle increases with a higher w/h-ratio. By deforming the molten polymer during the deposition through the nozzle, the molecular chains are oriented in the direction of extrusion. This is achieved by a plastic and an elastic component of deformation. When the pressure drops at the point the material leaves the nozzle, the elastic component recedes. This is phenomenon is described as relaxation and is, contrary to shrinkage, not a change in volume but a resetting of orientations. Therefore, only the shape may alter but the volume stays constant [8].

Table 4: Values for calculating the volume flow rate and the corresponding results.

Specimen	**1**	**2**
Length raster / contour lines / mm	3450.14	1950.19
Layer time / s (average value)	22.02	13.51
Print velocity / mm/s	156.67	144.33
Strand cross-section area / mm^2	0.086	0.152
Volume flow rate / mm^3/s	13.5	21.94

Based on this, the effect shown in Figure 10 may be explained with the relaxation increases with an increasing w/h-ratio and therefore an increasing volume flow rate which benefits the molecular orientation. The observation of the nozzle temperature during the manufacturing of the two specimens has shown that both specimens are built with an identical set nozzle temperature (315 °C), regardless of the different w/h-ratio and volume flow rate.

Previous investigations regarding the influence of deposition velocity related temperature deviations for the FDM process have shown that a higher volume flow rate at a constant nozzle temperature leads to a drop in temperature [9]. This drop in temperature may be the reason for the decrease of the geometric deviation with a further increase of the w/h-ratio and thereby the volume flow. The lower temperature levels lead to lower orientation of the molecules in the melt, therefore to a lower relaxation and finally to a lower geometric deviation.

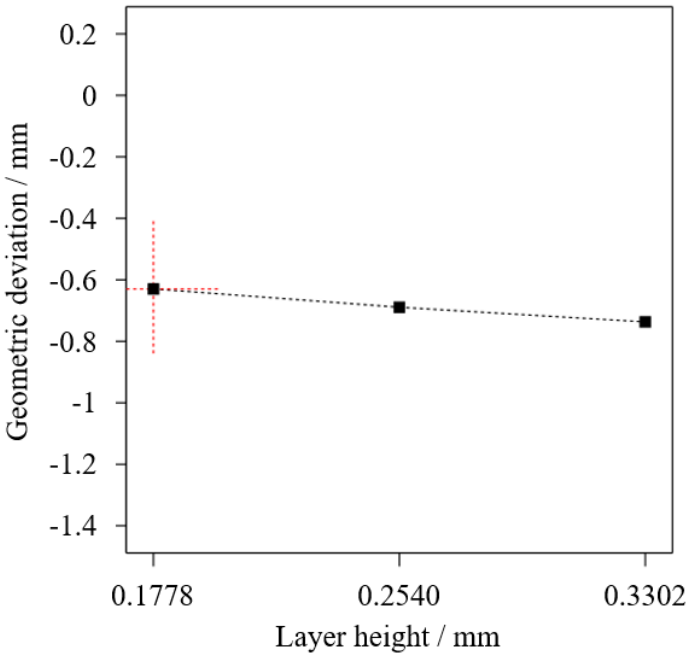

Figure 11: Effect of the layer height on the geometric deviation.

The results of the DoE show an influence of the layer height on the geometric deviations. With an increasing layer height, the geometric deviation also increases (see Figure 11). This can be explained with the strand bringing more thermal energy into the part at once. This provides more energy for the shrinking and relaxation to occur and therefore results in a higher geometric deviation. The reason for this effect being detectable regardless of the w/h-ratio is that the ranges of the strand cross-section area for the different layer heights do not overlap. The values shown in Table 5 indicate that with every increase in layer thickness in the DoE, the cross-sectional area is increasing no matter which w/h-ratio is chosen. The only exempt from this is between the layer heights of 0.2540 mm and 0.3302 mm. Here, the cross-sectional area of the strands for the layer height of 0.2540 mm and a w/h-ratio of 3 is larger than for the combination of 0.3302 mm and 1.7. The overlap in the cross-sectional area is 0.0064 mm^2 or 4.4 % and therefore, compared to the difference between the minimum and maximum cross-section area for the layer height of 0.3302 mm of 0.1113 mm^2.

Table 5: Comparison of the strand cross-sectional areas resulting from the different w/h-ratio and layer height combinations.

		Strand width / mm		Cross-sectional area/ mm^2	
w/h-ratio / -		1.7	3	1.7	3
Layer height / mm	0.1778	0.3023	0.5334	0.0422	0.0745
	0.2540	0.4318	0.7620	0.0861	0.1520
	0.3302	0.5613	0.9906	0.1456	0.2569

In Figure 12, the interactions between the factors air gap and w/h-ratio are shown. This is the only pairing of factors that shows an intersection of the curves. The model describes that with a low w/h-ratio the geometric deviation increases with a decreasing air gap. With a high w/h-ratio the geometric deviation decreases with a decreasing air gap. This can be explained with the increasing contact area between the layers induced by wider strands. These larger contact areas may be able to assist the suppression of shrinkage and relaxation by offering a

larger surface for the heat transfer and thus resulting in a more rapid cooling of the contact areas. By decreasing the distance between the strands, not only the contact area between two layers is enhanced but also the contact area between adjacent strands in the same layer. These contact areas may result in fixpoints for the newly deposited strand which then suppresses the shrinkage and relaxation. For the lower w/h-ratio this effect may not be visible as the absolute air gap value is lower for lower strand widths and therefore the contact area between the adjacent strands is smaller.

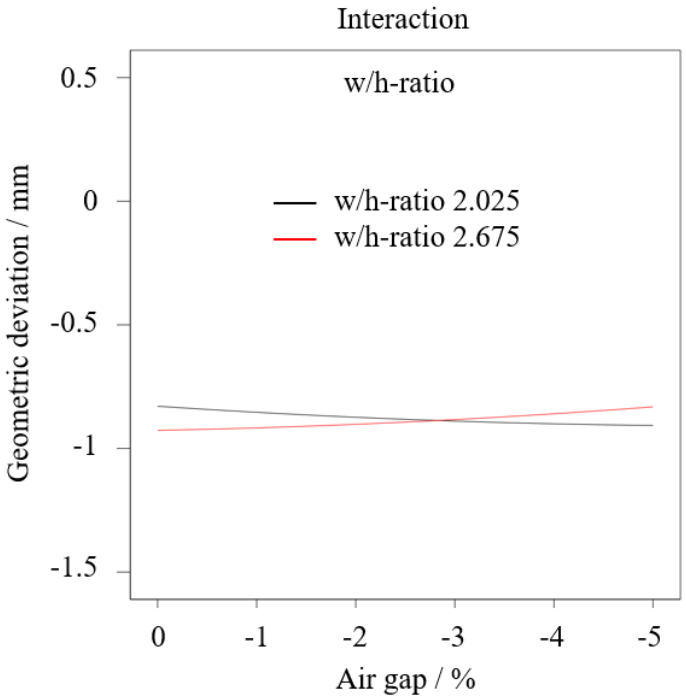

Figure 12: Effect of the interaction between the air gap and the w/h-ratio.

For the validation, at first, the fidelity of the model regarding the values the model is based on, is analyzed. The comparison of the predicted and the actual values is shown in Figure 13. The diagram includes three deleted values. Due to manufacturing errors these specimens were not considered for the model. In the diagram, five major accumulations of test point are visible. These mostly represent the five different nominal lengths for the most part. But especially values for the specimens with a nominal length of 102.5 mm are found in all three center groups. For the geometric deviations measured for the specimens with a nominal length of 200 mm, the values are scattering as the absolute effects of e.g. the layer height and raster angle are amplified.

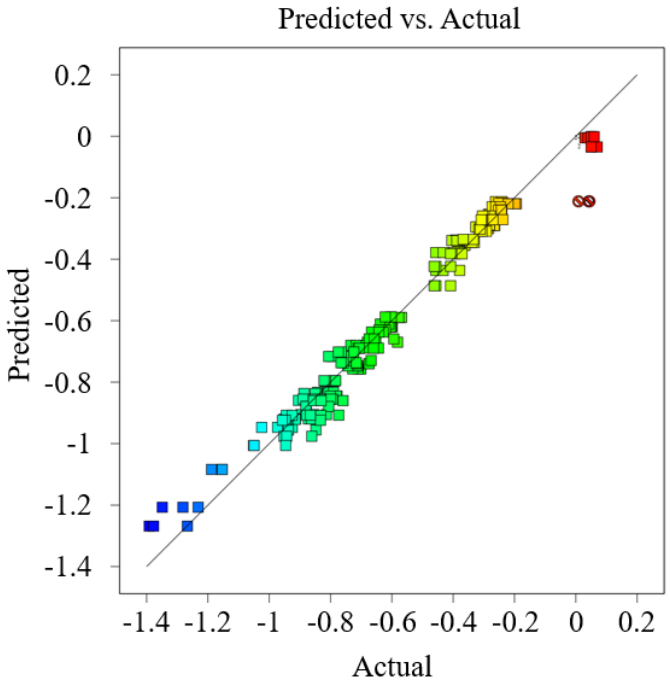

Figure 13: Comparison of the values predicted by the model and the actual values the model is based on.

Additionally, the model is validated using randomized process parameters for the manufactured specimens. The specimens were measured according to the previous procedure. The expected geometric deviation is calculated using the equation provided by the DoE software. In Figure 14 the results separated for the three different layer heights are shown. While the majority of the values is inside or close to the ±15 % tolerance, six values are not correctly predicted by the model. These specimens have a nominal length of 5 mm. The measurements for the specimens with a nominal length of 5 mm during the DoE have to be conducted with an outside micrometer at the moment. As in the FDM process sharp edges cannot be manufactured, certain deviations occur (see Figure 15). The cylinder of the outside micrometer has a diameter of 10 mm. Therefore, it cannot be assured that the geometric deviation in the center of the specimen is measured. The effect of the deviations in the corner areas of the specimens are considered in the model but do not represent the actual measurements.

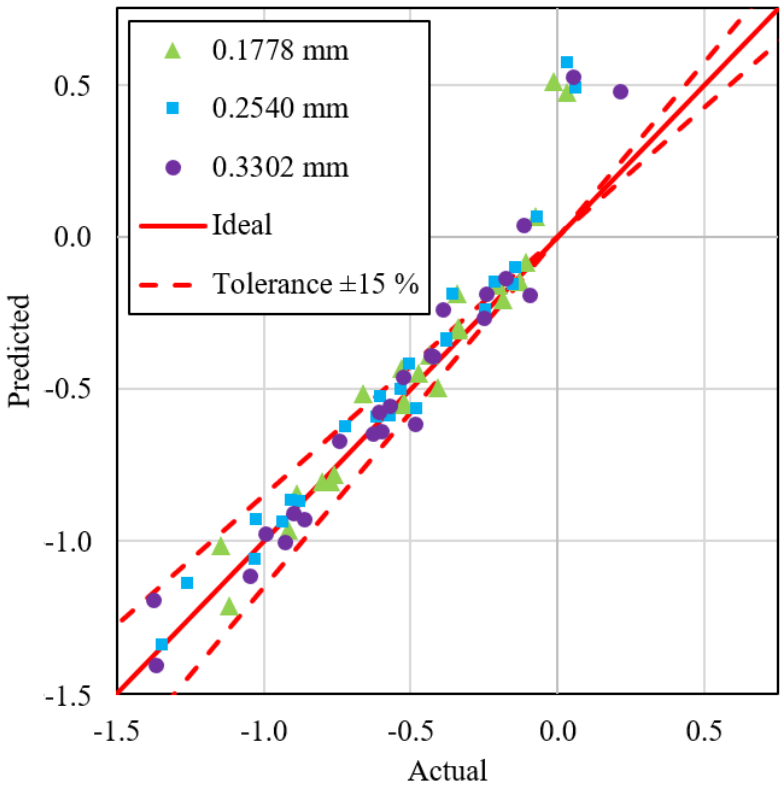

Figure 14: *Validation of the model using specimens built with randomized process parameters, broken down according to the individual layer heights.*

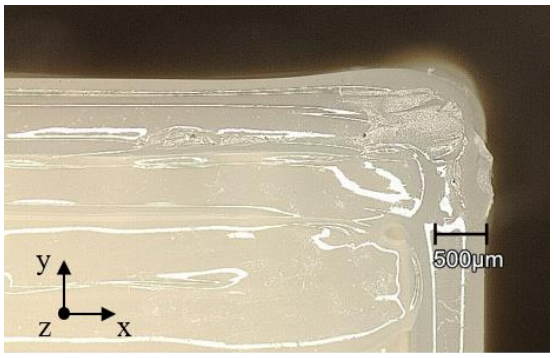

Figure 15: *Exemplary visualization of the deviations occurring on the edges of specimens manufactured in the FDM process.*

During the course of the investigations a curvature of the specimen surfaces oriented in z-direction is observed (see Figure 5). To further investigate this matter, specimens with a height of 30 mm are manufactured and measured according to Figure 6. The specimens are built using the process parameters shown in Table 2. The observation of the curvature during the conduction of the DoE is confirmed by the results of these investigations. The lowest deviation is seen in the bottom section of the specimens over all nominal lengths. It is assumed that this is due to the connection of these layers to the building platform, which restricts the materials ability to deform. The highest deviations were measured in the middle section. The measured values of the middle section are between those of the top and bottom section (see Table 6). A possible explanation is that due to the thermal energy input and the lacking heat transfer through

the part into the relatively cold building platform (build chamber temperature: 90 °C) the temperature level rises in the middle section and benefits the geometric deviations by enable the part to reduce residual stresses. These residual stresses build up when a hot strand is deposited onto an already solidified layer. The connecting points between these layers then function as fixtures resulting in residual stresses when the newly deposited material cools and shrinks.

The occurrence of residual stresses in the FDM process were described by *Wang et. al.* and *Li et. al.* Here, the focus was on the warpage behavior of specimens manufactured using the FDM process [10], [11].

Table 6: Average geometric deviation by position of specimens to investigate the curvature of surfaces oriented in z-direction.

	Average geometric deviation by section / mm		
Nominal length / mm	Bottom	Middle	Top
53.75	-0.3244	-0.3472	-0.3337
102.5	-0.6183	-0.6410	-0.6308
151.25	-0.9258	-0.9452	-0.9372
200	-1.1636	-1.1934	-1.1861

Form the middle sector upwards, the geometric deviation decreases. The reason for this may be that as no further material is deposited, the thermal input is reduced. This results in the top section not reaching the temperature level of the middle section for a sufficient time span. Therefore, the residual stress cannot be reduced by deforming of the layers.

Conclusion and Outlook

During the investigations a DoE was conducted to determine the influence of selected process parameters on the shrinkage behavior of raster lines in the FDM process. The results show that the nominal length is the most influential factor followed by the raster angle and layer height. The air gap itself does not have a significant influence on the geometric deviation. In combination with the w/h-ratio of the strands, effects are observable.

The model derived from the DoE was validated using specimens built with randomized process parameters. Except for specimens with a short nominal length, the model provides a sufficient representation of the measured values.

Further on, the curvature of the specimen surfaces oriented in z-direction has been identified. In a subsequent step the investigations were extended using specimens with a greater dimension in z-direction. These specimens too show identical behavior regarding the curvature.

Following the investigations presented in this paper, investigations regarding the individual effects observed with the DoE and are not yet explained without doubt, will be conducted. Also, the procedure will be transferred to different materials to identify possible parallels and eliminate the need to assess the shrinkage behavior of different materials in the FDM process by using adaption factors based on known materials.

Acknowledgement

The presented results were obtained in the context of the research project SCHO 551/0-1 “Simulation of the shrinkage behavior in Fused Deposition Modeling” sponsored by the Deutsche Forschungsgemeinschaft (DFG). We would like to thank the DFG for its support.

References

[1] Statista, „Meistgenutzte 3D-Drucktechnologien im Jahr 2021“, https://de.statista.com/statistik/daten/studie/760408/umfrage/ meistgenutzte-3d-druck-technologie/, 2021, last accessed 28.04.2022.

[2] S. S. Crump, “Apparatus and method for creating three-dimensional objects”, US005121329A, 1992.

[3] A. Gebhardt, “Additive Fertigungsverfahren. Additive Manufacturing und 3D-Drucken für Prototyping – Tooling – Produktion“, Carl Hanser Verlag, München, 2016.

[4] R. Dahlmann, E. Haberstroh, G. Menges: “Menges Werkstoffkunde Kunststoffe“, 7. Ausgabe, Carl Hanser Verlag, ISBN: 9783446458017, 2021.

[5] F. Knoop, “Untersuchung der mechanischen und geometrischen Eigenschaften von Bauteilen hergestellt im Fused Deposition Modeling Verfahren“, Shaker Verlag, Aachen, 2020.

[6] M. Bonnet, “Kunststofftechnik - Grundlage, Verarbeitung, Werkstoffauswahl und Fallbeispiele“, 3. Auflage, Springer Verlag, ISBN: 9783658138271, 2016.

[7] E. Baur, S. Brinkmann, T. A. Osswald, N. Rudolph, E. Schmachtenberg, „Saechtling Kunststoff Taschenbuch“, 31. Ausgabe, Carl Hanser Verlag, ISBN: 9783446434424, 2013.

[8] C. Bonten, “Kunststofftechnik - Einführung und Grundlagen“, 3. aktualisierte Auflage, Carl Hanser Verlag, ISBN: 9783446464711, 2020.

[9] E. Moritzer, F. Hecker, J. Wächter, F. Knaup, “Investigation of the Deposition Velocity Related Temperature Deviations for High Temperature Materials in the FDM Process”, 37th International Conference of the Polymer Processing Society, Fukuoka, Japan, 2022.

[10] T.-M. Wang, J.-T. Xi, Y. Jin, “A model research for prototype warp deformation in the FDM process“, The International Journal of Advanced Manufacturing Technology, Volume 33, Issue 11, pp. 1087-1096, Springer, 2007.

[11] H. Li, T. Wang, Q. Li, Z. Yu, N. Wang, “A quantitative investigation of distortion of polylactic acid (PLA) part in FDM from the point of interface residual stress”, The International Journal of Advanced Manufacturing Technology, Volume 94, Issue 1, pp. 381-395, Springer, 2018.